

Chapter - IV

Magnetisation Study

4.1 INTRODUCTION :

The nature of application of a ferrite is decided by its hysteresis studies which furnish an invaluable data on the permeability μ , the saturation magnetisation M_s , the coercive force H_c and the remanence ratio $\frac{M_r}{M_s}$ (Fig.4.7). The wide range of permeability values of ferrites make them suitable for various frequency range applications. The coercive force varies from 0.1 Oe upto 3000 Oe. The ferrite can be classified into two groups, on the basis of coercive force H_c . The ferrite with low H_c are called as soft ferrites, where as with high H_c are called as hard ferrites, Soft ferrites are used in the manufacture of high frequency inductances, cores of transformers, motors and generators. The overall requirements of these applications are high permeability, low coercive force, and small hysteresis losses. Hard Ferrites are generally used as permanent magnets. Electric motors, loud speakers, telephones, TV and other applications, also need high remanence. Neel in 1949 has shown that the coercive force. H_c is related with the crystal anisotropy, the saturation magnetisation, the internal stresses and the Porosity⁽¹⁾ of the material. Hysteresis properties are highly sensitive to crystal structure, heat treatment, chemical constitution, porosity and grain size⁽²⁾ etc. The preparation of ferrites with good squareness of loop characteristics demands most stringent conditions and atmosphere.

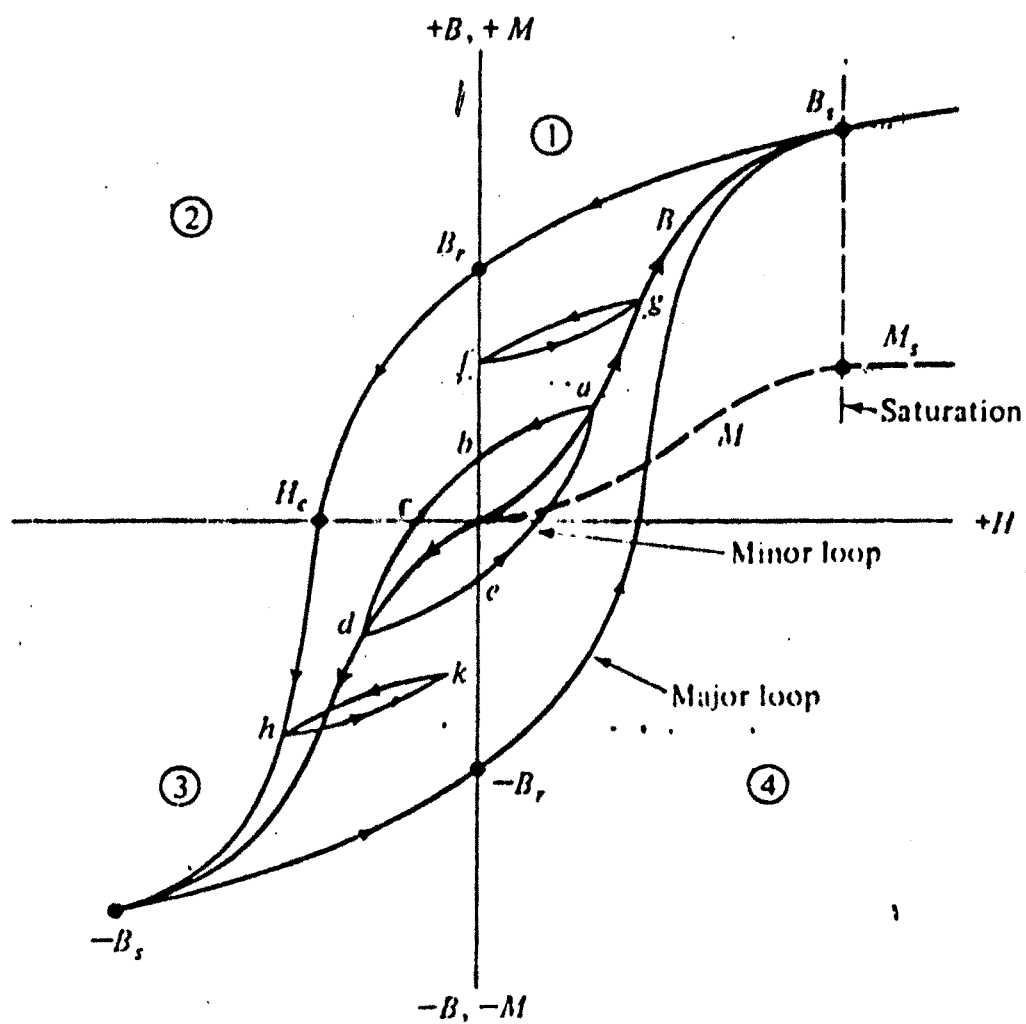


Fig. 4-7

The saturation magnetization is an important basic magnetic property of ferrite which can be measured by ballistic method⁽³⁾ the vibrating coil magnetometer^(4,5) vibrating sample magnetometer^(6,7) and microwave methods.^(8,9) We have been obtained saturation magnetisation for slow cooled and Quenched Ferrite System $\text{Cu}_x \text{CO}_{1-x} \text{Fe}_2 \text{O}_4$ ($0 \leq x \leq 1$) from hysteresis loop by using high field loop tracer HS 869 supplied by Electronics Corporation of India.

A brief survey of the theory pertaining to the Phenomenon of hysteresis is presented in this chapter in order to make use of this theory for the discussion of obtained results .

4.2 THEORETICAL ASPECTS :

The spontaneous magnetisation was first explained by Weiss (1907)^(10,0) by postulating the existence of molecular field. However the fact that ferromagnetic crystals frequently exhibit the state of Zero magnetisation led , to the prediction of randomly obtained domains.

According to Barkhusen⁽¹¹⁾, the change in magnetisation is discontinuous for the continuously changing applied field. This supported the interpretation that the magnetisation is due to rotation of magnetisations of the whole domains. Landu and Lifshitr showed that, domain formation in any ferromagnetic material is a consequence of considerable reduction in magnetostatic energy from that of the saturation magnetisation.

The attempt was made to overcome limitations^{of} Weiss molecular field theory by Heisenberg (1928)⁽¹²⁾. He gave quantum mechanical treatment to explain alignment of moments in terms of exchange interaction between the un-compensated spins of electrons in the partially filled 3-d shells. He showed that under certain conditions the exchange energy produces effects similar to those of Weiss molecular field. In this case electrons with parallel spins have lower energy than those with antiparallel alignments. Spontaneous magnetisation can also arise as a result of negative exchange interactions under favourable conditions of intervening ions. Neel⁽¹³⁾ in 1948 showed that in this case, the neighbouring magnetic moments are antiparallel. This is the origin of spontaneous magnetisation in ferrites where there are magnetic moments arranged in antiparallel or some other complex fashion compensating partially. The magnetic moments contributing to the magnetisation are mainly spin magnetic moments due to the quenching of orbital angular momentum. The non-integral values of the magneton numbers in case of Fe, Ni, Co at 0°K could not be explained by the Heisenberg model but has been explained on the basis of band theory of solids (Stoner 1933)⁽¹⁴⁾.

The exchange energy is given by

$$W_{ex} = 2Js^2 \sum_{i \neq j} \cos \theta_{ij}$$

Where : S the total spin momentum per atom.

θ_{ij} the angles between spin momentum vectors of atoms i and j.

Here anisotropy is neglected and only nearest neighbour exchange interactions are considered.

The ferrimagnetic and antiferromagnet materials had been investigated by extending the basic **concepts** associated with the explanation of ferromagnetic materials .

Neel developed theory of antiferromagnetism and ferrimagnetism by assuming the two sub-lattice model. Also he suggested the possibility of antiparallel alignment of spins of nearest neighbours in contrast to the parallel alignment in the ferromagnetism.

According to Neel's theoretical contribution to the antiferromagnetism and ferrimagnetism was proved experimentally first by Gorter (1950) and also by Guillaud (1949, 1950, 1951).⁽¹⁵⁾

According to Neel's two sub-lattice model, antiferromagnetism can be explained by quantum mechanical exchange interaction⁽¹⁶⁾. The antiferromagnetism may be regarded as a special case of ferrimagnetism in which magnetic moments of two sub-lattices are antiparallel and identical in magnitudes lead to net zero magnetisation. In ferrimagnetism, magnetic moments of two sub-lattices are antiparallel but they differ in magnitude lead to net magnetisation. The difference in magnitude attributed due to

one, different spin magnetic moments are either magnetic ions of sub-lattice, two different crystallographic sites that may be occupied by the magnetic ions.

Neel theory had been extended by Yafet and Kittel⁽¹⁷⁾ by assuming triangular arrangement of spin, in which A-A and B-B interactions are comparable in magnitude to the A-B interaction.

4.3 MAGNETIC ANISOTROPY :

The term 'anisotropy' is generally referred to describe "directional dependence" of some physical properties like elasticity and strength which are markedly dependent on crystallographic direction.

The anisotropy energy (magnetocrystalline energy) is the difference between the energy required to magnetize the samples to saturation along the hard direction and that required along an easy direction. This energy is dependent upon orientation of magnetization with respect to crystallographic axis. For ferrites which are cubic crystals, the anisotropy energy is given by

$$W_k = K_1(\alpha_1^2 \alpha_2^2 + \alpha_2^2 \alpha_3^2 + \alpha_3^2 \alpha_1^2) + K_2 \alpha_1^2 \alpha_2^2 \alpha_3^2 + \dots$$

Where K_1 and K_2 are the anisotropy constants characteristics of the particular material and $\alpha_1, \alpha_2, \alpha_3$ are the direction

cosines of magnetisation vectors with respect to the cubic axes.

When the crystal is strained there is change in the anisotropy energy which is called the magneto-elastic energy W_{λ} . It is due to change in interatomic spacing. One more contribution to the energy is that of magnetostatic energy W_M which is the work required to assemble all the dipoles constituting the body. The magnetostatic energy needs to be reduced which occurs as a result of division of crystal into domains. This subdivision halts at a point where the energy required for the formation of an additional domain wall becomes greater than the decreases in the magnetostatic energy.

Bloch⁽¹⁸⁾ in 1932 has shown that the change in the magnetisation between two neighbouring domains takes place over a finite width. If it has to occur over a unit interatomic distance very high value of exchange energy would be required. This wall of finite width contains spins whose orientations gradually change from the direction in one domain to that in the other. Thus the atomic spin within the wall do not remain parallel to an easy direction and so lead to some anisotropy energy.

There are two types of walls— 180° walls and 90°

walls. The spins rotate by 180° from one domain to the other in the former case and by 90° in the latter case. The thickness of the domain wall is determined by the condition of minimum total energy. It is given by $\sigma = \left(\frac{A}{K} \right)^{\frac{1}{2}}$ this leads to wall energy $W_r = 4/(AK)^{\frac{1}{2}}$

Where A is the exchange energy constant and K is anisotropy constant⁽¹⁹⁾ In principle the optimum domain configuration can be determined from the condition of minimum free energy i.e. by minimising $W = W_{ex} + W_k + W_\lambda + W_m + W_r$ for particular value of applied field. The shape of the magnetisation curve for a crystal can be determined by repeating this procedure for the various values of the applied field, but in practice it is different.

It is seen that a Bloch wall appears when there is a transition of magnetisation from a given direction to any other under the condition of zero-divergence of magnetisation across the wall.

When the thickness of the specimen is small, of the order of the width of the domain wall, the interaction between the strips of free poles formed at the intersections of the wall with the specimen surface becomes important. This was first pointed out by Neel⁽²⁰⁾ in the year 1935. He predicted a new type of transition. The wall is called a Neel wall. Here the magnetisation rotates from one domain to the neighbouring

one while remaining in the plane of the film. In case of the films (thin specimens) Neel walls become energetically favoured. This work has been extended by middlehoek⁽²¹⁾ where in the energy for different transitions is given as a function of angles between orientations of neighbouring domains.

There is one more type of spin transition in which the wall is called crossed tie wall. Here the short right angled cross-ties are regularly arranged. This structure is explained by considering the variation of the closure of flux at alternate intervals through the plane of spin rotation around the spiraling axis of the wall.

Middlehoek⁽²²⁾ in 1963 has shown that the energy of a wall of cross-tie type is roughly 0.6 times the energy of Neel wall. From the theory it appears that Bloch wall is formed in specimens of thickness greater than approximately 900\AA and for specimen with thickness less than about 900\AA , cross tie wall is most favoured, according to these theoretical consideration Neel wall is not expected to be formed at all. However, in specimens of thickness less than about 200\AA Neel walls are observed.

Experimentally more complex walls have been observed where spin rotations are complex, such walls may consist of alternate section of pure Bloch type of transitions and pure

Neel type of transitions with region of complex combinations of both types in between the two to achieve continuity.

For polycrystalline material with grains that not very small the domain structures for each grain are roughly similar to those in large crystals of course there will be modifications in the domain structure due to small dimensions of the grains and due to interaction between adjacent grains results in case of polycrystalline ferrite are similar to those as observed for single crystal.

4.4. IRREVERSIBILITY AND HYSTERESIS :

Generally irreversibility and hysteresis in ferromagnetic materials are attributed to impediments to the motion of domain walls offered by defects like inclusion, heterogeneities due to other phase and dislocations⁽²³⁾ magnetisation proceeds by reversible wall motion and at very high fields by irreversible rotations. Above the threshold field, Barkhausen jumps are observed in magnetisation when the wall energy is maximum. This leads to irreversible increases in magnetostatic and magnetoelastic energies of the material under the action of external magnetic field. When the magnetic field is reduced to zero the residual magnetisation remains locked the thermal energy required for randomisation and wall motion not being available. Also during magnetisation reversal nucleation has to proceed

before the sequence of reversible and irreversible wall motion and spin rotation can take place. Therefore for a unisolated specimen the changes result in hysteresis during the magnetisation cycle, signifying the energy loss. A model of wall motion proposed by Kersten⁽²⁴⁾ in 1943 for an inhomogeneous material having non magnetic inclusion considers changes in the energy of the domain wall due to variations of the area of the wall.

The strain and the inclusion theories considered only plane domain walls and regular arrays of imperfection and also did not deal with the magnetic disturbance created by the imperfection. However, in view of the statistically distributed imperfections, the number of imperfections that will be intersected by the wall on an average would remain the same. This does not portend a variation in the wall energy leading to small coercivity. Further work on the problem led Neel to establish that there are variations in the magnitude and direction of the magnetisation due to the randomly distributed irregularities within the same domain. From this dispersed field theory Neel calculated critical field required for irreversible moments of domain wall and coercivity.

4.5 L_O_S_S_E_S_:

When a magnetic material is used in an alternating magnetic field a certain portion of the magnetic energy is

absorbed by the material and dissipated as heat. In an alternating field is $H = H_0 \exp(i\omega t)$ then the induction B can, in general be represented as

$$B = B_0 \exp i (\omega t + \delta) \dots \dots \quad (4.1)$$

So that

$$\begin{aligned} \mu &= \frac{B}{H} \\ &= B_0 / H_0 (\cos \delta + i \sin \delta) \\ &= \mu' + i \mu'' \dots \dots \end{aligned} \quad (4.2)$$

Where μ' gives that component of the flux which is in phase and μ'' the one that is 90° out of phase with the applied field. The energy loss per cycle can be shown proportional to μ'' . The ratio $\frac{\mu''}{\mu'}$ = $\tan \delta$ is called power factor or loss factor. The quality factor 'Q' is defined as

$$Q = \frac{\mu'}{\mu''} = \frac{1}{\tan \delta} \dots \dots \quad (4.3)$$

From the point of view of application the variation of μ' and μ'' against frequency is an important criterion and is called magnetic permeability spectrum.

The important mechanism of losses are (1) hysteresis (2) eddy current (3) spin resonance (4) relaxation and (5) wall resonance. For ferrites working at low fields the hysteresis and eddy current losses are relatively small, and the major contribution comes from the remaining sources.

4.5.1 HYSTERESIS LOSS:

The energy dE required to change magnetisation M to $M+dM$ at a field H is given by $dE = HdM$. Thus the total energy absorbed for a complete hysteresis cycle is

$$W = \oint HdM \quad \dots\dots\dots (4.4)$$

Which is equal to the area under the hysteresis loop, Low coersivity or high permeability results in a small area under the loop and hence a small loss.

4.5.2 EDDY - CURRENT LOSS:

An electric current is induced in the magnetic core material by the alternating magnetic field. This causes heating and power loss. It is found that the power loss per second is proportional to $\frac{2AF^2}{\rho}$ where F is the frequency and ρ the electrical resistivity of the core material, the constant of proportionality depending upon the geometry of the core.

4.5.3 SPIN RESONANCE LOSS:

Under the influence of the internal anisotropy field H_k the electron spin vector in a magnetic material processes with frequency ω given by $\omega = \gamma H_k$ where γ is the gyromagnetic ratio. If the electron spin vector subjected to an external r-fmagnetic field H_i in a direction perpendicular to that of

Hk, then the resonance sets in, when the radio frequency matches the precession frequency and energy is absorbed from the applied field in case of a material with negative crystal anisotropy constant the rotational processes are important, then the resonant frequency is inversely proportional to $(\mu-1)$. Therefore, when the permeability of the material is higher the resonant frequency is lower.

4.5.4 RELAXATION LOSS :

The loss that is exhibited at frequencies much lower than the resonance frequency needs to be accounted for. This has been attributed to several relaxation processes. The major relaxation loss in ferrites is attributed to the electron exchange between Fe^{2+} and Fe^{3+} ions, As the magnetisation changes its direction, then Fe^{2+} and Fe^{3+} ions tend to change their position to attain the configuration that has the lower energy under the changed direction of magnetisation. The readjustment of the Fe^{3+} , Fe^{2+} position does not require movement of ions but merely that of electrons.

This relaxation loss is frequency dependent and is maximum when the applied frequency is close to the relaxation frequency for electron jump for a given material at a given temperature.

4.5.5 WALL RESONANCE LOSS :

In certain samples, the low frequency loss has been identified as due to domain wall resonance. If the domain wall is disturbed from its equilibrium position, a restoring force sets in, which tries to bring it back. The wall like a stretched membrane, thus has a natural frequency of oscillation. If the frequency of the applied magnetic field matches this natural frequency, resonance absorption sets in.

4.6 EXPERIMENTAL :

4.6.1 A P P A R A T U S :

High field 100p tracer Hs 869 supplied by Electronic corporation of India Limited, Hyderabad was used for the measurements on hysteresis (plate c). It consists of an alternating current electromagnet working on 50Hz with the aid of which a sinusoidal field of maximum peak 3500 oe is produced in about 9mm air gap. The instrument operates on 230 volts 50Hz a.c. A special balancing coil is used to deflect the magnetisation of the sample placed in the air gap.

The signal from the balancing coil after integration is proportional to the magnetic moment of the specimen and is fed to the vertical plates of an oscilloscope after suitable amplification.

The signal from the balancing coil is also used to deflect the

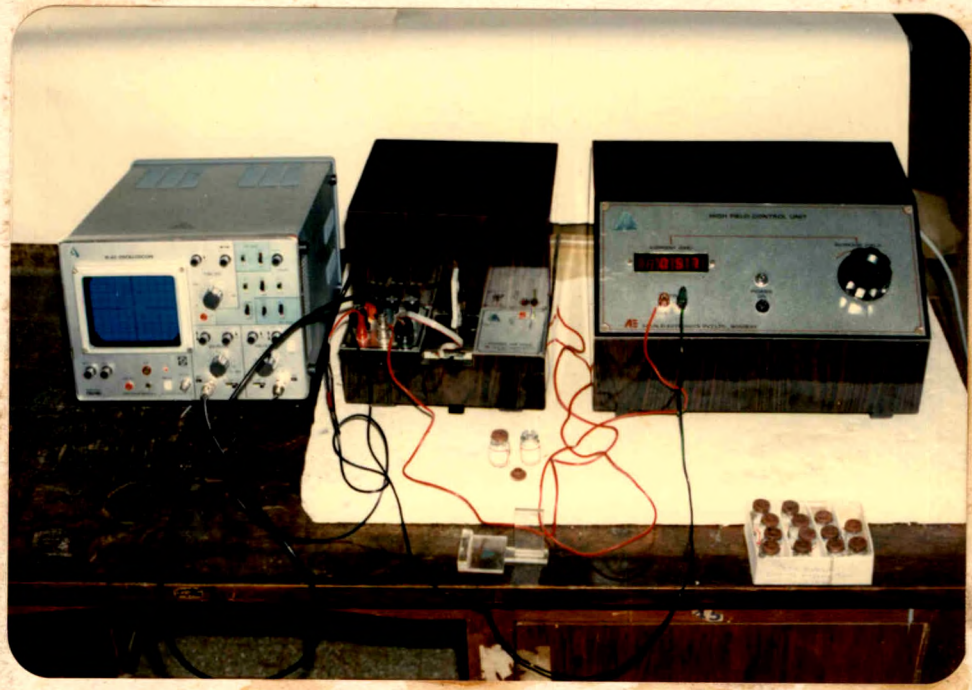


(Plate c)

A signal proportional to the magnetic field is fed to the horizontal plates of the oscilloscope. Thus the oscilloscope displays magnetic moment versus field, that is, hysteresis loop for the sample. The vertical deflection can be calibrated in terms of magnetic moment in e.m.u. and horizontal in Oe per division. The magnetic parameters are accurate to within 5%.

4.6.2 MEASUREMENT PROCEDURE :

The measurement of M_s value was carried out directly from the C.R.O. screen which was properly illuminated and calibrated, before introducing the sample in the balancing coil in the core space, the stray fields, stray signals and phase mismatch were carefully got rid of with the aid of controls provided. Even after introducing the sample the set up was once again tested for the above mentioned interferences when the current in the electromagnet was zero. Then the current was gradually increased and the hysteresis loop was obtained on the C.R.O. screen. The divisions of the C.R.O. on Y-axis (magnetisation axis) were calibrated using the standard Ni strip, having the saturation magnetisation is 53.34 emu/gm.

For the measurement of M_s by hysteresis loop on C.R.O. screen, a digital multimeter was connected across the vertical deflection of C.R.O. and reading in millivolts was

was noted for every ferrite sample and also for standard Ni-sample.

4.7. RESULT AND DISCUSSION :

In figure (4.1) the compositional variation of magnetic moment (nB) in Bohr magneton is given. It is seen that as content of copper i.e. x is increased the magnetic moment of the system $\text{Cu}_x \text{Co}_{1-x} \text{Fe}_2 \text{O}_4$ decreases. A linear decrease is exhibited by this compositional variation except for the ferrite $\text{Cu}_{0.6} \text{Co}_{0.4} \text{Fe}_2 \text{O}_4$. The value of nB is maximum for $\text{Cu}_{0.2} \text{Co}_{0.8} \text{Fe}_2 \text{O}_4$ and minimum for $\text{Cu}_{0.8} \text{Co}_{0.2} \text{Fe}_2 \text{O}_4$.

In fig (4.2) the compositional variation of saturation magnetisation is shown, almost similar trend is depicted by this variation. In table No.1 the values of saturation magnetisation, magnetic moments, and curie temperatures and cation distribution for the slow cooled samples of the system $\text{Cu}_x \text{Co}_{1-x} \text{Fe}_2 \text{O}_4$ are reported.

The experimental values of magnetic moments are calculated using the relation-

$$nB = \frac{\text{molecular weight} \times \sigma_s}{5585 \times ds}$$

$$\sigma_s = \text{emu/gm.}$$

$$Ms = \text{emu/cm}^3$$

TABLE NO. 1
SLOW COOLED SAMPLE

Sample	σ_s	n_B	$\frac{M_r}{M_s}$	Tc	Cation distribution
$Cu_{0.2}Co_{0.8}Fe_2O_4$	105	2.27	0.42	455	$(Cu_{0.076}Fe_{0.924})^A(Cu_{0.124}Co_{0.8}Fe_{1.076})^B O_4^-$
$Cu_{0.4}Co_{0.6}Fe_2O_4$	57	1.6	0.32	447	$(Cu_{0.168}Fe_{0.832})^A(Cu_{0.232}Co_{0.6}Fe_{1.168})^B O_4^-$
$Cu_{0.6}Co_{0.4}Fe_2O_4$	53	1.53	0.37	440	$(Cu_{0.264}Fe_{0.736})^A(Cu_{0.336}Co_{0.4}Fe_{1.264})^B O_4^-$
$Cu_{0.8}Co_{0.2}Fe_2O_4$	25	0.72	0.37	432	$(Cu_{0.368}Fe_{0.632})^A(Cu_{0.432}Co_{0.2}Fe_{1.368})^B O_4^-$

TABLE NO. 2
 QUENCHED AT 600°C

Sample	σ_s	n_B	$\frac{Mr}{Ms}$	Tc	Cation distribution
$Cu_{0.2}Co_{0.8}Fe_2O_4$	112	3.0	0.41	440	$(Cu_{0.088}Fe_{0.912})^A(Cu_{0.112}Co_{0.8}Fe_{1.088})^B O_4$
$Cu_{0.4}Co_{0.6}Fe_2O_4$	84	2.35	0.37	420	$(Cu_{0.184}Fe_{0.816})^A(Cu_{0.216}Co_{0.6}Fe_{1.184})^B O_4$
$Cu_{0.6}Co_{0.4}Fe_2O_4$	76	2.22	0.33	418	$(Cu_{0.282}Fe_{0.718})^A(Cu_{0.318}Co_{0.4}Fe_{1.282})^B O_4$
$Cu_{0.8}Co_{0.2}Fe_2O_4$	27	0.79	0.42	413	$(Cu_{0.384}Fe_{0.616})^A(Cu_{0.416}Co_{0.2}Fe_{1.384})^B O_4$

TABLE NO. 3
 QUENCHED 800°C

Sample	σ_s	n_B	Mr/Ms	Tc experimen- tal	Cation distribution
$Cu_{0.2}Co_{0.8}Fe_2O_4$	122	3.32	0.36	445	$(Cu_{0.084}Fe_{0.916})^A(Cu_{0.116}Co_{0.8}Fe_{1.084})^B O_4$
$Cu_{0.4}Co_{0.6}Fe_2O_4$	87	2.37	0.27	426	$(Cu_{0.18}Fe_{0.82})^A(Cu_{0.22}Co_{0.6}Fe_{1.18})^B O_4$
$Cu_{0.6}Co_{0.4}Fe_2O_4$	82	2.37	0.28	423	$(Cu_{0.276}Fe_{0.724})^A(Cu_{0.324}Co_{0.4}Fe_{1.276})^B O_4$
$Cu_{0.8}Co_{0.2}Fe_2O_4$	28	0.82	0.5	420	$(Cu_{0.384}Fe_{0.616})^A(Cu_{0.416}Co_{0.2}Fe_{1.348})^B O_4$

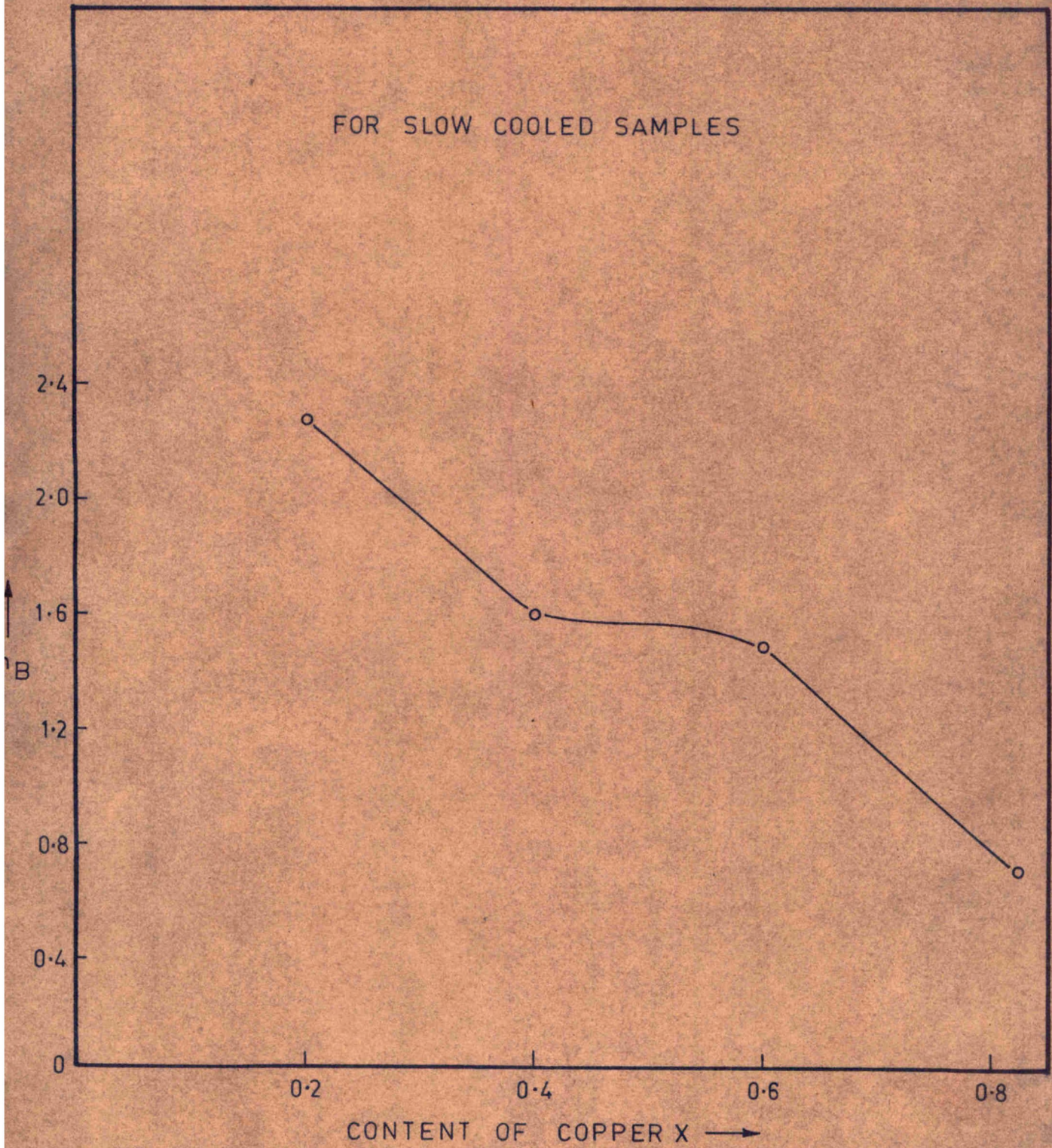
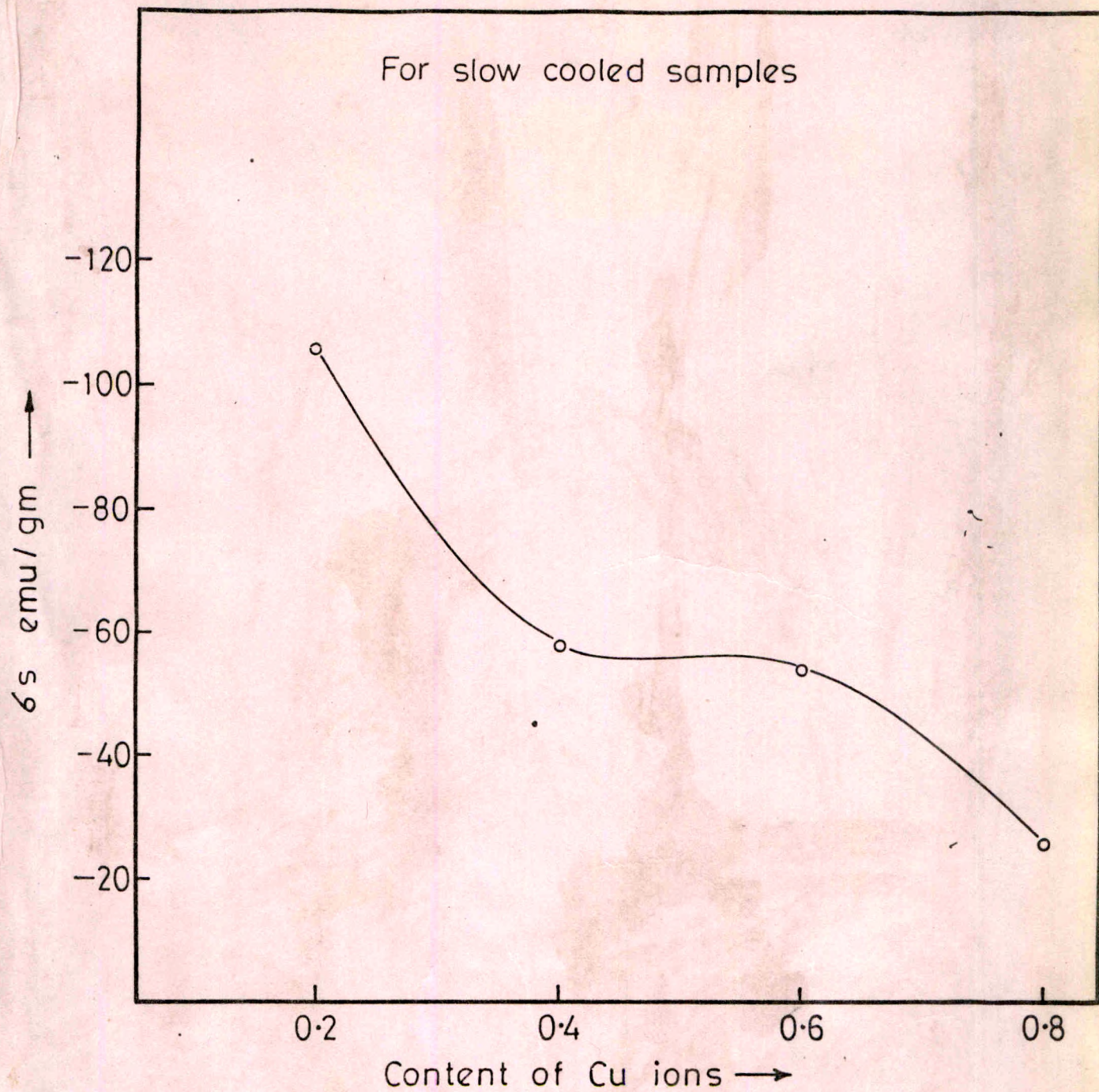


Fig.4.1 VARIATION OF η_B vs CONTENT OF COPPER X .



THE COMPOSITIONAL VARIATION OF SATURATION
MAGNETISATION vs CONTENT OF COPPER X.

Gilleo has also given the expression for T_c as

$$T_c = \frac{3\lambda(1-\lambda) f(\lambda, m) g(\lambda, m) m T_0}{2((1-\lambda) f(\lambda, m) + \lambda g(\lambda, m))}$$

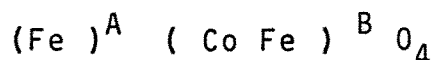
Where

$$f(\lambda, m) = 1 - (1 - \lambda m)^5 (1 + 5\lambda m) \dots \dots \dots (4.6)$$

$$g(\lambda, m) = 1 - (1 - \frac{1}{2}m(1 - \lambda))^{11} (1 + \frac{11}{2}m(1 - \lambda)) \dots \dots \dots (4.7)$$

and $T_0 =$ a constant (in K)

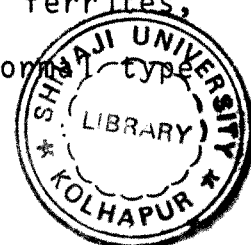
We have evaluated $T_0 = 793^\circ \text{K}$ by assuming that $\text{Co Fe}_2 \text{O}_4$ has cation distribution of the type.



For which $T_c = 520^\circ \text{c}$

The decrease in the magnetic moment with the increase in content of Cu can be explained on the basis of cation distribution.

Then saturation magnetisation in ferrites is determined by physicochemical constitution and also by the cation distribution and other attendant aspects of thermophysical history of ferrites. In case of ferrites the solid solubility affords to prepare mixed ferrites, crystallising in the spinel structure either of normal type or of inverse type.



Where d_s is the density and M_s is calculated using the relation.

$$M_s = (1-P) \sigma_s d_s$$

Where P is porosity, σ_s is saturation magnetisation emu/gm the porosity was calculated using the relation.

$$P = \frac{\text{X-ray density} - \text{actual density}}{\text{X-ray density}}$$

The cation distribution is computed from the experimental values of the curie temperature (T_c) using Gilleo's formula.

Gilleo has given cation distribution for a general spinel system.

$$M_{3-m} Fe_m O_4 \quad (0 < m < 3) \text{ as}$$

$$Fe_m M_{1-m\lambda} (Fe_{(1-\lambda)m} M_{2-(1-\lambda)m}) O_4 \quad \dots (4.4)$$

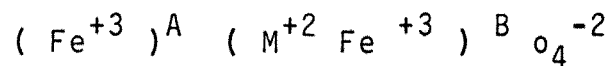
Where M is non-magnetic ion and λ is cation distribution coefficient .

For our present system $m = 2$ and hence formula (4.4) becomes.

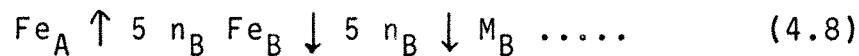
$$Fe_{2\lambda} M_{1-2\lambda} (Fe_{2(1-\lambda)} M_{2\lambda}) O_4 \quad \dots (4.5)$$

The two sub-lattice model applied to the spinel structure in order to explain the magnetisation of ferrites has been successful to a large extent.

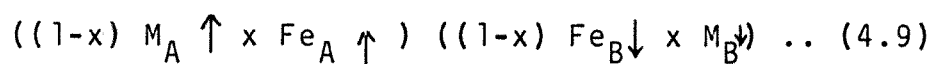
For the ferrite with inverse spinel structure such a formula is



The Fe^{+3} ions on A site are coupled with their spins antiparallel to those of Fe^{+3} ions on B-site, so that the net moment is only due to divalent M^{+2} metallic ions.



suppose that M is a transition element with n electron in d shell, the magnetic moment μ_B per unit formula is $n \mu_B$ or $(10-n) \mu_B$ depending on d shell which is filled less than half or more than half respectively. The degree of inversion is a fraction x of the divalent metal ions that are on B-site. The arrangement of moments could be written as



The net moment μ_B is written as

$$\begin{aligned} \mu_B &= (M(1-x) - x) - 5 (1 + (1-x) - x) \\ &= M(1-2x) - 10(1-x) \dots\dots \quad (4.10) \end{aligned}$$

For normal spinel $x=0$

inverse spinel $x=1$

The A-B exchange interaction in a spinel ferrite are strengthened by the addition of strong magnetic ion and weakened by the addition of ~~weak~~ magnetic ion.

Thus value of n_B is decided by the transition of Cu^{+2} ions Fe^{+3} ions present on A-site. Addition of Cu pushes some of Fe^{+3} ions from B site to A site. Also $CuFe_2O_4$ is partially inverted ferrite and when Cu^{+2} is substituted in a system there is migration of Cu^{+2} ions to A-site migration of Fe^{+3} ions from A to B site leads to increase of magnetic moments however substitution of Co by Cu results in the decrease of magnetisation. The net result is the reduction in M_s .

The sample $Cu_{0.4}Co_{0.6}Fe_2O_4$ however shows a disproportionate decrease in the value of n_B which may be attributed to the occurrence of unstable phases like Co_3O_4 $CoFe_2O_4$ or $CuCoFe_2O_4$ during the process of cooling.

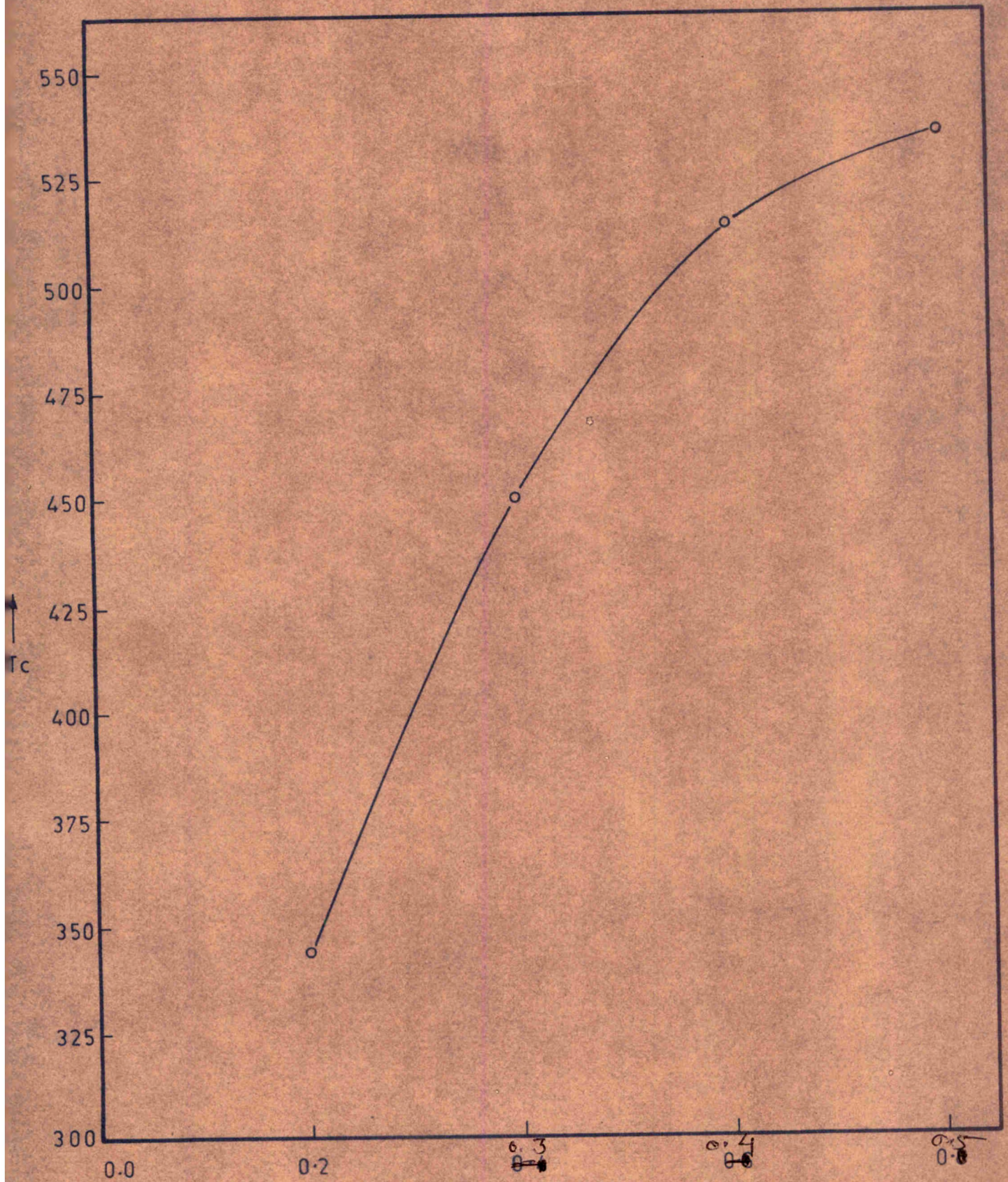
In fig.(4.3) the theoretical values cation distribution parameter versus (T_c) is given. This variation used to compute the cation distribution of the system.

In fig.(4.4) the compositional variation of the experimental values of curie temperature(T_c) is given. It is seen that with the addition of Cu the curie temperatures are lowered in a linear fashion. T_c is maximum for $Cu_{0.2}Co_{0.8}Fe_2O_4$ while, it is minimum for $Cu_{0.8}Co_{0.2}Fe_2O_4$. This linear variation suggest that in the present system co-linear

Theoretical values of cation distribution

Parameter λ vs T_c (°K)

140



~~COMPOSITION OF COPPER λ~~
Theoretical cation distribution parameter λ
Fig. 4.3

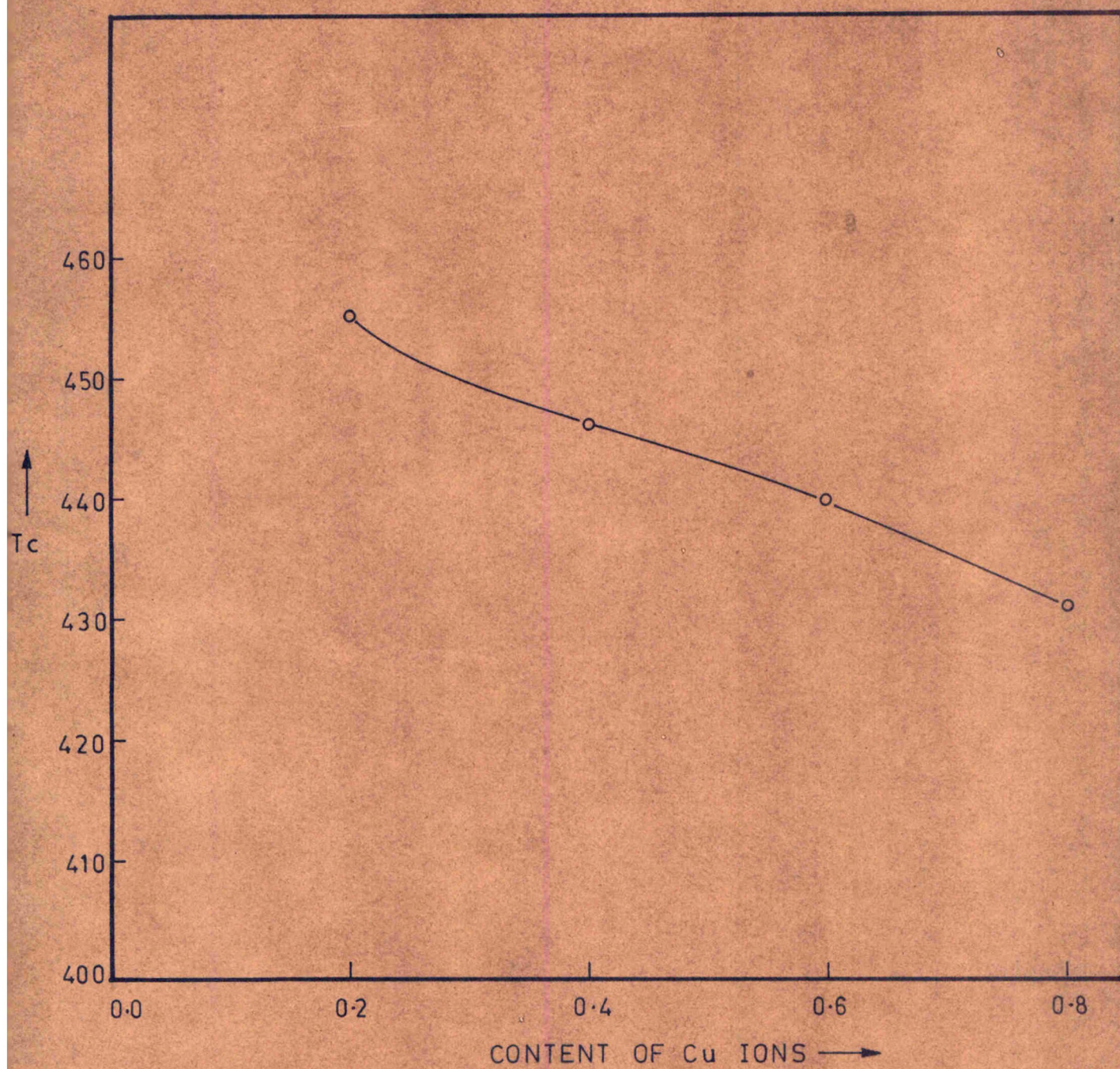


Fig.4-4 VARIATION OF EXPERIMENTAL T_c vs CONTENT OF Cu IONS.

types of spin arrangement are favoured. This fact is corroborated by the zero yafet-kittle angle shown by our samples. Hence we have applied Neels two sublattice model for the explanation of magnetisation to our systems.

In fig(4.5) compositional variation of the squareness ratios $\frac{M_r}{M_s}$ is shown. It is seen that as content Cu is increase from $x= 0.2$ to $x= 0.5$ a decreasing trend is exhibited by M_r / M_s variation while as content of Cu is increase from $x=0.5$ to $x= 0.8$ and increasing behaviour is observed in case of M_r / M_s variations. M_r / M_s depends on factors like impurities, defects, polarizable constituent and other hindrance to the domain wall motion. The decrease of $\frac{M_r}{M_s}$ ratio suggest that there is less impedance to domain wall motion. However with the substitution of Cu, The ions having more magnetic moments that is cobalt are being replaced by the ions having less magnetic moment. Hence there is a trend towards reduction in the both M_s and M_r and this trend may be responsible for more decreasing M_r than that in case of M_s up to 50% content of Co. The variations of M_r/M_s appeared to be governed by the presence of Co because the trend in M_r/M_s and magnetisation there one to one **correspondence** as far as compositional variation is concerned. However in case of samples containing Cu in excess of 50% the M_r/M_s shows interesting increase in trend. It can be concluded that this compositional variation of M_r/M_s is dominated more by Cu ions. Thus when copper substituted in excess of 50% in the ferrite $Cu_x Co_{1-x} Fe_2 O_4$ the impedance

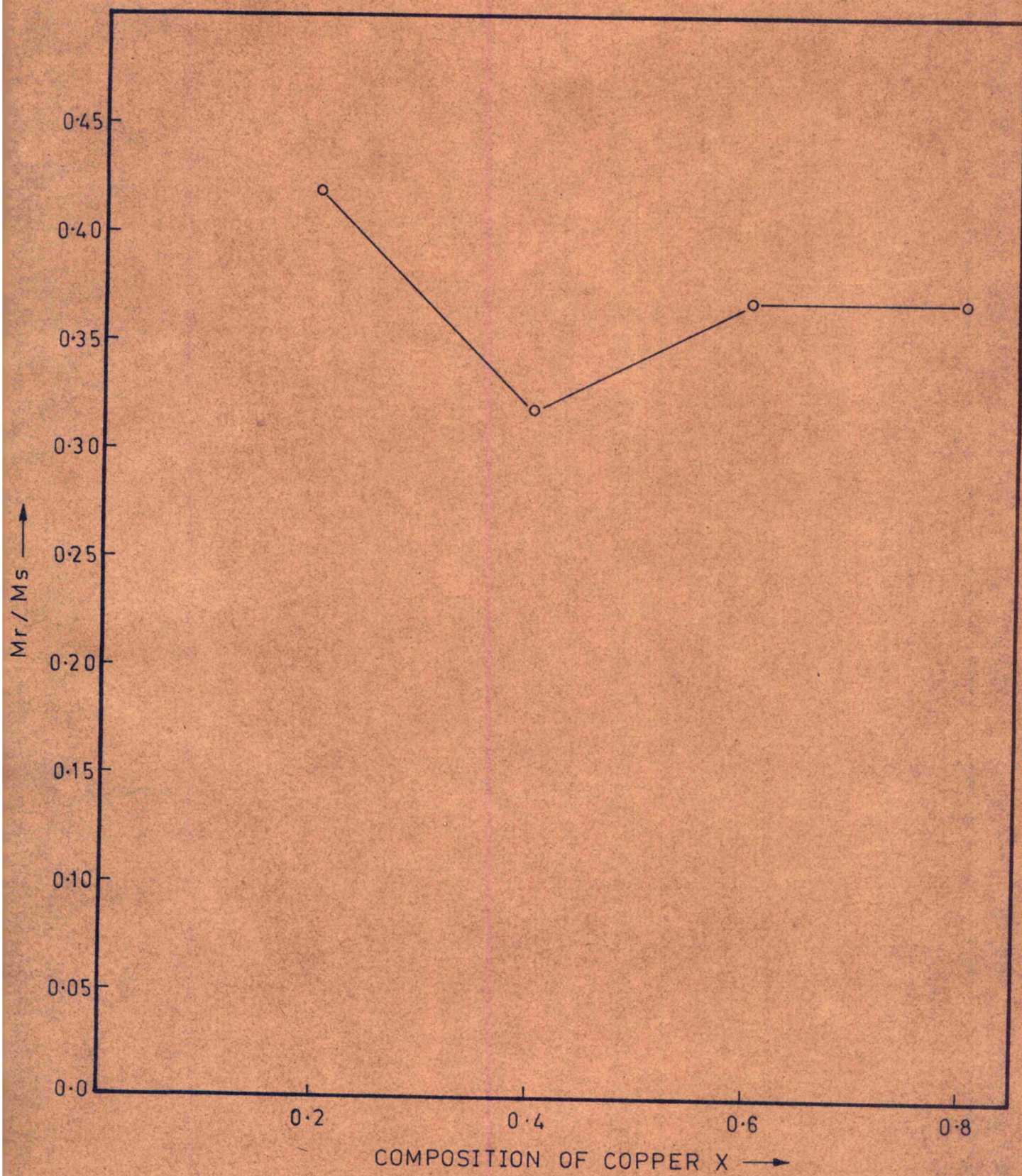


Fig. 4.5 Mr/Ms RATIO vs COMPOSITION OF COPPER X .

to the domain wall motion is increased.

144

In fig (4.6) variation of nB with the temperature of quenching is shown for $Cu_x Co_{1-x} Fe_2 O_4$ samples. All the samples exhibit similar trend of variation, for slow cooled samples the values of nB are minimum while they increase gradually as the temperature of quenching is increased.

$CuFe_2 O_4$ exhibits electrical switching⁽²⁵⁾ changing semiconductive properties⁽²⁶⁾ and tetragonality variation⁽²⁷⁾ when heat treat under different condition.

Copper ferrite has low resistivity but positive seebeck coefficient, When quenched ~~from~~^{at} high temperature,

Semiconductive properties of copper ferrite ^{can} be corelated not only with oxidation state but also with cation distribution.

It is well known that $MgFe_2 O_4$ also exhibits properties sensitive to heat treatment similar to $CuFe_2 O_4$ ferrite, $CoFe_2 O_4$ ferrite is completely inverse⁽²⁵⁾ and does not show changing properties on quenching.

The observed change in nB for the slow cooled and quenched samples can be explained by considering that at

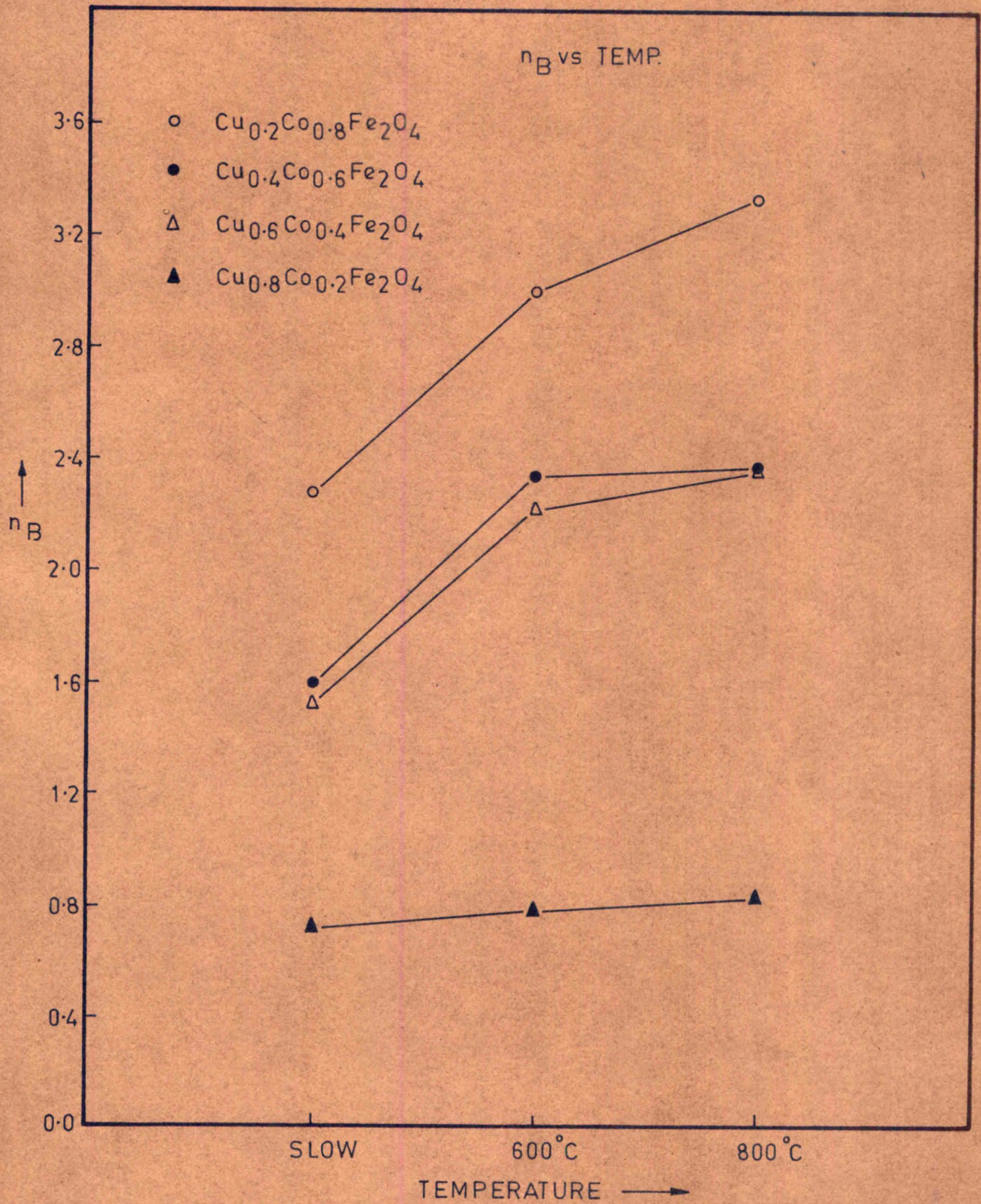


Fig. 4.6

elevated temperature, the cation distribution between A and B sites becomes random and is frozen on quenching these samples.

From Table No. 1,2,3 it is seen that more the temperature of quenching more is the migration of Cu^{+2} ions to A sites. These ions push equal amount Fe^{+3} ions to B site and increase the magnetisation.

R E F E R E N C E S :

1. C.M. Srivastava, M.J. Patani and T.T. srinivasan, 'Effect of Jahn- Teller' ion on the ground states of Fe and Ni ions in spinel ferites' J.Appl.phys. 53(3) (1982) P.2107.
2. E.Sterm, 'Microwave, material and applications', Jr.of Applied phys.vol.38, No.3 P.1397-99(1967).
3. L.F. Bates, Modern magnetism C.U.P.P. 5(1951).
4. D.O.Smith, Rev.Sci.Instr 27.P.261(1956).
5. D.Fidman and R.P. Hunt, Z.Instrument Kunde 72,P.259 (1964).
6. S.Foner Rev.Sci.Instr.27 P 584 (1956)
7. S.Foner & E.J.MicNife Rev.Sci.Instr,39,P171(1968)
8. C.Kittel, phys.Rev,73 P.155(1948).
9. H.Brand and H.W.Fieweger, Proc.IEEE 53 P.186(1965).
10. Weiss,P, "L Hypothese du champ molecularie ef la properite ferro magntique' J.de.physique,6,661(1907).

11. Barkhausen, H. "Two phenomena covered with the help of the new amplifiers" phys.zeits 20,401. (1919)
12. Heisenberg W. "on the theory of ferromagnetism" zeit fur phys.49,619(1928).
13. Neel L. "magnetic properties of ferrites" ferrimagnetism and antiferrimagnetism, Ann physique 3, 137 (1948).
14. Stoner, E.C. "Atomic moments in ferromagnetic metals and alloys with non-ferromagnetic elements" phil.mag 15 1018(1933)
15. Lux and Button, microwave ferrites and ferrimagnetism Mc Grawhill Book company Inc.P.No.4 (1962)
16. Allen H.morrish "The physical principles of magnetism" John wiley and sons Inc. (1965)
17. Y.Yafet and C.Kittel, Antiferr magnetic arrangements in ferrite phys.Rev.vol.87 P.290 (1952).
18. Bloch F. "Theory of exchange problem and of residual ferromagnetism" zeit fur phys.74,(1932) P.295.
19. Sinha A.P.B.and Menon P.G. solid state chemistry marcel Dekker, INC,N.Y. (1974).

20. Neel L "Energies es puros de Bloch dans ICS couches minces" *Compt Rend Acad Sci. paris* 241 (1955) P.533.
21. R.Carry and E.D. Issac, magnetic Demain and techniques for their observation, The English univ. press Ltd. London E.C. 4 (1966).
22. Middlehoek 5" Domain walls in their Ni-Fe Films" *J. Appl.phys* 34(1963) P.1054.
23. Kondorsky E. "on the nature of the coersive force and irreversible changes in magnetisation" *physik z. 50W-jetunion* 1,(1937) P.597.
24. Keroten M." Grundlagen ciner Theorie der ferromagnetischen Hysteresese under kuerzihvkraft Hirzel Leipzig (1943).
25. ~~Winkler G magnetic properties of material edited by~~
Winkler G.magnetic properties of amterial edited by J. Smith (Megraw Hill New York) (1971) 22.
26. Nanba N & Kobayashi K,*Jpn J Appl phys (Japan)* 17 (1978) 1819
27. Yamashiro T. *Japn J. Appl phys (Japan)* 12 (1973) 148.